Interaction of oxygen with Au/Ti(0001) surface alloys studied by photoelectron spectroscopy

2010 J. Phys.: Condens. Matter 22 265002

(http://iopscience.iop.org/0953-8984/22/26/265002)

J. Phys.: Condens. Matter **22** (2010) 265002 (7pp) doi:10.1088/0953-8984/22/26/265002

Interaction of oxygen with Au/Ti(0001) surface alloys studied by photoelectron spectroscopy

N Tsud[1,4], F Šutara[1,5], I Matolínová[1], K Veltruská[1], V Dudr[2], K C Prince[3] and V Matolín[1]

[1] Faculty of Mathematics and Physics, Department of Surface and Plasma Science, Charles University, V Holešovičkách 2, 18000 Prague 8, Czech Republic
[2] Institute of Physics, Academy of Sciences of the Czech Republic, Cukrovarnická 10, 16200 Prague, Czech Republic
[3] Sincrotrone Trieste, Strada Statale 14, km 163.5, I-34149 Basovizza-Trieste, Italy

E-mail: tsud@mbox.troja.mff.cuni.cz

Received 3 December 2009, in final form 21 April 2010
Published 24 May 2010
Online at stacks.iop.org/JPhysCM/22/265002

Abstract
The interaction of oxygen with gold adsorbed on Ti(0001) was studied by synchrotron radiation photoelectron spectroscopy. Two kinds of surfaces were explored: as-deposited 0.38, 1.16 and 1.85 monolayer (ML) thick Au overlayers on the Ti(0001) surface, and the same samples after thermal treatment, which resulted in the formation of Au–Ti intermetallic surfaces. The Ti 3p core level was strongly affected by reaction with oxygen, while the Au 4f core level showed only minor changes other than a decrease in intensity. The Ti 3p peak was fitted with several components which were identified as Ti atoms in different oxidation states, namely TiO, Ti_2O_3, TiO_2 and Ti–OH. Titanium oxide phase formation is accompanied by Au–Ti bond dissociation and outward diffusion of Ti. The presence of an Au–Ti intermetallic phase on the Ti(0001) surface promotes oxidation of the Ti atoms.

(Some figures in this article are in colour only in the electronic version)

1. Introduction

Oxidation of Ti metal has continued to attract the attention of the scientific community due to the practical importance of titanium oxide. The range of Ti oxide applications is extremely wide, for instance in heterogeneous catalysts, gas sensors, solar cells, protective coatings and the aerospace industry; it is also used in biomaterials owing to the biocompatibility of Ti-oxide-based implants with human tissue and bones [1–3]. Titanium is an early transition metal with a low filling of the d-band (nominally two electrons). Oxygen readily interacts with titanium metal, which results in the existence of several stable Ti oxidation states, for instance TiO, Ti_2O_3 and TiO_2, of which the most stable is TiO_2, with titanium in the preferred oxidation state of +4.

In many cases alloying of Ti with various metals, instead of pure titanium, improves the properties of both titanium and its surface oxide for chemical, mechanical and biological applications [2, 3]. Ti6Al4V alloy is one of the most promising compounds suitable for the majority of biomedical applications, particularly for implants due to its excellent biocompatibility. Thermal oxidation of the Ti6Al4V alloy and commercially pure Ti at high temperatures (1120 K) was studied by Zhang *et al* [4]. It was shown that pre-deposited gold on the Ti6Al4V and Ti surfaces promotes oxygen adsorption and results in the formation of a thicker titania layer compared with conventional thermal oxidation. The presence of a thin gold layer (hundreds of nanometres) was shown to be beneficial for the outward diffusion of titanium during thermal oxidation.

In order to gain insight into the mechanism of titanium oxide formation and into the role of Au–Ti alloying we have studied O_2 adsorption on ordered Au/Ti(0001) surface alloys. The main goal was to investigate the effect of O_2 exposure

[4] Author to whom any correspondence should be addressed.
[5] Present address: Physics Department, CINVESTAV-IPN, Avenue IPN 2508, 07360 Mexico, DF, Mexico.

at 300 K on the electronic structure of the Au/Ti(0001) surface alloy by photoelectron spectroscopy using synchrotron radiation.

The present study builds on our previous work on Au–Ti well-defined bimetallic surfaces of Ti(0001) [5]. The Au/Ti(0001) adsorption system was studied by low energy electron diffraction and photoemission spectroscopy with synchrotron radiation. Formation of an intermetallic interface and associated valence orbital hybridization, together with diffusion of gold into the bulk, was observed. For step-wise Au adsorption on the Ti(0001) surface at 300 K, no additional superstructures were observed. Annealing of the 1.7 ML Au/Ti(0001) surface at 670 K gave rise to a $(\sqrt{3} \times \sqrt{3})$R30° structure, and upon further annealing at 670 K a stable (2×2) surface reconstruction appeared. By raising the temperature to 720 K and annealing for a few minutes, another ordered phase of the Au/Ti(0001) interface formed, described as a one-dimensional incommensurate reconstruction with a rectangular $(\sqrt{3} \times \sqrt{3})$ unit cell. The Au 4f core level and valence band photoemission spectra provided evidence of a strong chemical interaction between gold and titanium.

2. Experimental details

The experiment was performed at the Materials Science Beamline, at the Elettra synchrotron light source in Trieste. The UHV experimental chamber, with a base pressure of 1×10^{-10} mbar, was equipped with a 150 mm mean radius electron energy analyser, rear-view LEED optics, electron beam evaporation Au source and an ion gun.

The photoemission spectra were taken at a photon energy of 148 eV. The total resolution was determined by measuring the width of the Fermi level at a temperature of 120 K and was equal to 130 meV. At this temperature the intrinsic width of the Fermi level is 40 meV so we estimate the resolution of the photons + analyser to be about 125 meV. The spectra were recorded at normal emission of the photoelectrons with respect to the surface. The intensities of the photoelectron spectra were normalized to the incident photon flux. The Au $4f_{7/2}$ core levels were fitted by a convolution of a Gaussian and a Doniach–Sunjic lineshape with subtraction of a Shirley-type background.

The titanium sample was a disc of 12 mm diameter and 3 mm thickness, with a large grain oriented to within 0.1° of the (0001) plane. The grain was mapped by translating the sample in front of the LEED and using the edges of the sample as reference points. Then the sample was illuminated by synchrotron light and the photoemission spectra measured after translating by appropriate distances to find the correct coordinates of the (0001) grain. The cleaning procedure consisted of many cycles of ion sputtering and annealing at 920 K.

3. Results

3.1. Au evaporation rate

To calibrate the deposition rate, the Au $4f_{7/2}$ photoemission intensity was measured as a function of evaporation time at low temperature (120 K), with the aim of inducing layer-by-layer growth. The intensity grows initially with a single $4f_{5/2}$–$4f_{7/2}$ doublet at low coverage, and then after 8 min, a second doublet appears at lower binding energy. The Au $4f_{7/2}$ core level intensities as a function of the evaporation time are plotted in figure 1(a). The Au $4f_{7/2}$ core level intensity was decomposed into two peaks Au(I) and Au(II) by curve fitting. The fitting parameters used were as in [5], with a Lorentzian width of 0.32 for both components, while the Gaussian width was allowed to vary to optimize the fit (it was in the range of 0.37–0.47 eV for Au(I) and 0.70–0.36 eV for Au(II)). The area of the Au $4f_{7/2}$ peak components is plotted in figure 1(b) as a function of deposition time. For the Au(I) intensity, a plateau was observed after about 8 min of deposition time, while for Au(II) only a gradual signal increase was found. The Au(I) feature is assigned to Au at the Au/Ti interface, and for increasing gold coverage it becomes less visible. The binding energy (BE) of the Au $4f_{7/2}$ (I) peak (84.34 eV) is close to the BE value for the Au/Ti(0001) intermetallic surfaces of 84.5–84.6 eV reported in [5]. We conclude that at 120 K the Au/Ti(0001) interface has intermetallic character although surface ordering did not occur (no LEED pattern was observed). At this temperature, it is reasonable to believe that diffusion into the bulk was also suppressed. We attribute the low binding energy component Au(II) (figure 1(a)) of the Au $4f_{7/2}$ core level to Au that is bonded to other Au atoms, i.e. on-top of the first Au/Ti(0001) intermetallic interface, which may be a discontinuous layer or clusters. The plateau intensity of the Au $4f_{7/2}$ (I) peak component was considered as the signal which corresponds to 1 ML of Au, where 1 ML is defined as coverage equal to the number of Ti atoms in the topmost layer of the clean surface. (The metallic diameters of Au and Ti are very similar, 0.2884 and 0.2896 nm, respectively.)

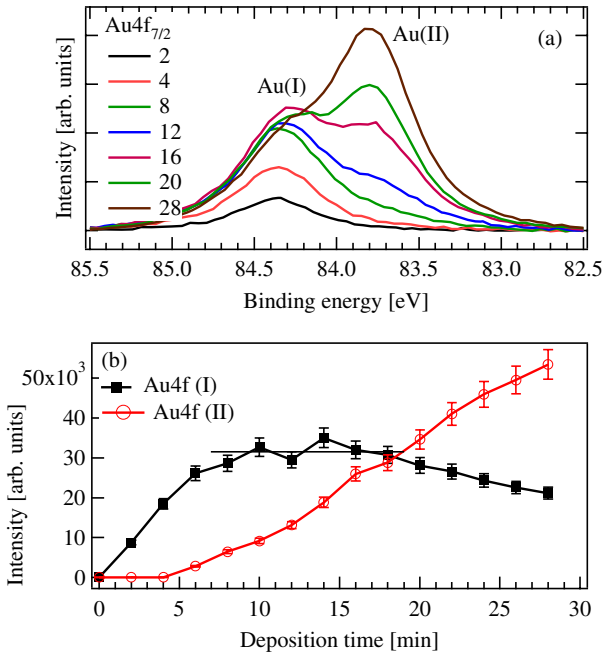

Figure 1. (a) Au $4f_{7/2}$ core level intensity as a function of evaporation time; sample at 120 K. (b) Au $4f_{7/2}$ area of Au(I) and Au(II) fitted components versus deposition time.

Table 1. Names and description of samples with amount of deposited gold (in ML) on the Ti(0001) surface.

Sample name	Treatment	Coverage, LEED
s1	—	0.38 ML, weak (1 × 1)
s2	—	1.16 ML, no spots
s3	—	1.85 ML, no spots
s4	0.38 ML, 570 K, 1 min	0.35 ML, weak (1 × 1)
s5	1.16 ML, 670 K, 2 min	0.54 ML, $(\sqrt{3}\times\sqrt{3})$R30 + (2×2)
s6	1.85 ML 670 K, flash	0.84 ML, $(\sqrt{3}\times\sqrt{3})$R30

3.2. O_2 adsorption

The interaction with oxygen was studied for Ti(0001) surfaces with the following Au coverages: 0.38, 1.16 and 1.85 ML deposited at 300 K (labelled s1, s2 and s3); and substrates with the same amount of gold after flashing or annealing to 570 or 670 K (labelled s4, s5 and s6). Parameters of the sample preparation, including flashing and annealing conditions, are summarized in table 1. The thermal treatment resulted in the formation of Au–Ti intermetallic surfaces with different composition and ordering (for details see table 1). After exposure of these surfaces to 10 L O_2 at 300 K, the Ti 3p, Au 4f and O 2s core levels and valence band spectra were recorded.

The Ti 3p core level spectra before and after O_2 exposure for all Au/Ti(0001) surfaces together with the oxygen exposed clean Ti(0001) surface are shown in figure 2. The spectra of the s3 surface do not show any change after oxygen adsorption and this sample was not considered for further analysis. Dosing of other samples by oxygen resulted in prominent changes of the spectra. Ti 3p spectra after O_2 exposure of the Ti(0001), s1, s2, s4, s5 and s6 samples together with fitted components described later are presented in figures 3 and 4. The shape of the Ti 3p core level is complicated by the presence of a satellite at higher binding energy than the main peak. To avoid ambiguity in curve fitting, we subtracted the clean metal spectrum after suitable normalization from the spectrum after oxygen adsorption. The clean metal spectrum was suitably scaled to get the best overlap of background and the low binding energy edge of the Ti 3p peak for each considered spectrum; then the metal contribution was subtracted from the spectra. Figures 3 and 4 show Ti 3p spectra after oxygen adsorption together with the curves where the Ti or Au–Ti contribution was subtracted. The latter spectra were fitted with several components in order to model the Ti atoms in different oxidation states. A Gaussian lineshape with subtraction of a Shirley-type background was used for all components and the fits were found to give good agreement with the measured data. The best fit for the Ti(0001) surface consists of five peaks (p0, p1, p2, p3 and p4), whereas for all Au/Ti(0001) intermetallic surfaces only four components were distinguished. The binding energies and Gaussian widths of the components are listed in table 2 compared with the BE values for a thick TiO_2 film on SiO_2 [6] and a TiO_2(110) crystal [7]. The Ti 3p components were assigned to Ti atoms in different bonding states: Ti metal or Au–Ti surface alloy (subtracted before fitting), TiO, Ti_2O_3, TiO_2 oxide and Ti–OH, labelled p1, p2, p3 and p4 in figures 3 and 4, respectively.

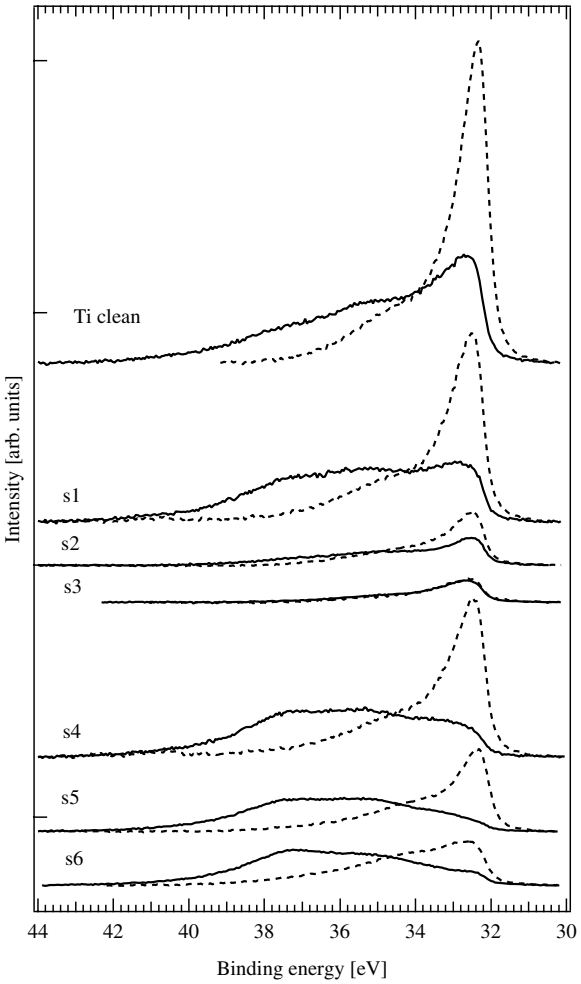

Figure 2. Ti 3p core level before (dashed line) and after 10 L O_2 adsorption (solid line) on the clean Ti(0001), s1–s6 surfaces measured at 148 eV photon energy.

For the O_2/Ti(0001) surface, the extra component p0 was attributed to chemisorbed oxygen atoms on the Ti surface. This assignment will be discussed further below. The ratio of O_2-induced intensities of Ti 3p to the total Ti 3p intensity after 10 L exposure was considered (see table 2, values in brackets). It can be seen that the major part of the Ti 3p intensity is redistributed between the Ti_2O_3 and TiO_2 peaks. For all considered Au/Ti(0001) surfaces the TiO_2 peak dominates the oxygen-induced components, whereas for the clean Ti(0001) surface the Ti_2O_3 peak is slightly higher compared to the TiO_2.

The Gaussian widths of the Ti 3p peak increase monotonically from p0 to p4 for all samples, and there are two possible causes. We exclude lifetime effects because the number of d electrons decreases from p0 to p4, which would increase the Auger lifetime, and believe the widths are due to heterogeneity. The trend can also be seen as an increase in width with oxidation state, or width of the gap. Metals have a zero gap, Ti_2O_3 is a semiconductor and stoichiometric TiO_2 is a wide gap insulator. We explain the variation in width by pinning of the Fermi level at different points in the gaps of the higher oxidation phases. Compositions with stoichiometries close to TiO are metallic [8], and so in this case

Table 2. Binding energies and Gaussian widths (Gw, in eV) of the Ti 3p core level components labelled p1, p2, p3 and p4 in figures 3 and 4. The values in brackets are the relative intensity with respect to the total Ti 3p intensity after 10 L O_2 exposure. The data for the oxidized Ti(0001) crystal are shown for comparison. The binding energy uncertainty is less than 0.05 eV.

O_2 10 L on	Ti or AuTi	TiO_{ads} (p0)	TiO (p1)	Ti_2O_3 (p2)	TiO_2 (p3)	Ti–OH (p4)
Ti (0001) or s0	—	32.67	33.30	34.72	37.04	39.49
	—	Gw 0.64	Gw 1.20	Gw 2.54	Gw 3.08	Gw 3.50
	(0.19)	(0.06)	(0.13)	(0.30)	(0.25)	(0.07)
s1	—	—	33.39	34.76	37.06	39.8
	—		Gw 1.13	Gw 2.28	Gw 3.17	Gw 3.6
	(0.27)		(0.07)	(0.21)	(0.38)	(0.07)
s2	—	—	33.54	34.94	36.97	39.5
	—		Gw 1.12	Gw 1.95	Gw 3.1	Gw 3.4
	(0.62)		(0.02)	(0.11)	(0.24)	(0.01)
s4	—	—	33.38	34.96	37.20	39.71
	—		Gw 1.34	Gw 2.25	Gw 2.80	Gw 3.34
	(0.15)		(0.09)	(0.27)	(0.40)	(0.09)
s5	—	—	33.28	34.97	37.26	39.43
	—		Gw 1.22	Gw 2.43	Gw 2.77	Gw 3.66
	(0.08)		(0.06)	(0.33)	(0.41)	(0.12)
s6	—	—	33.81	35.08	37.15	39.5
	—		Gw 1.35	Gw 1.86	Gw 2.71	Gw 3.45
	(0.24)		(0.04)	(0.17)	(0.44)	(0.10)
TiO_2/SiO_2, [6]	—	—	—	—	37.8	—
TiO_2(110), [7]	—	—	—	—	37.5	—
TiO_2, [11]	—	—	—	—	38.0	40.0

the broadening may be due to variations of local stoichiometry. This explanation may also apply in part to the other phases.

An example of the O 2s core level at a binding energy of 22.5 eV is shown in figure 5(a) for the s5 surface; the energy positions of the peak for other surfaces remain the same with only a difference in intensity. The measured O 2s binding energy values for the oxidized Au/Ti(0001) surfaces agree rather well with the published data for related systems, namely thick TiO_2 film on the SiO_2 substrate, for which a BE value of 22.6 eV was reported [6]. The O 2s signal for all samples after 10 L O_2 adsorption is plotted in figure 5(b). The absolute amount of oxygen uptake is maximum for the s4 surface, i.e. for the Au/Ti(0001) intermetallic surface with the lowest amount of gold atoms. At the same time, the relative contribution of the TiO_2 component to the Ti 3p signal has a maximum for the s6 surface (see table 2), where the amount of the initially deposited gold is maximum, and which by annealing to 670 K resulted in a subsurface layer rich in Au atoms.

The O 2s to the total Ti 3p peak area ratio versus Au coverage is presented in figure 6. It can be seen that the value decreases for the 'untreated' surfaces (s1, s2 and s3), for which higher Au coverage causes a reduction in the oxygen adsorption ability of the Ti atoms. For all intermetallic Au/Ti(0001) surfaces, independent of the Au coverage, the O 2s to Ti 3p ratio is the same, 1.32 ± 0.5. We conclude that the amount of adsorbed oxygen is proportional to the number of top-surface Ti atoms alloyed with gold.

Apart from the intensity change, the Au 4f core level was only slightly influenced by the adsorption of oxygen for all Au/Ti(0001) surfaces. Figure 7 represents the Au $4f_{7/2}$ core level for the s4 and s6 samples before and after oxygen adsorption, for which the biggest peak shape change was observed. For as-deposited Au adlayers (s1, s2 and s3) and sample s5, mainly an intensity decrease was detected with minor peak shape change; the spectra are not shown. The Au/Ti(0001) intermetallic surface with lowest coverage of gold (s4) shows broadening of the Au $4f_{7/2}$ peak after 10 L O_2 exposure with a small shoulder at about 84 eV binding energy. For the surface with the highest surface and subsurface Au concentration (s6), the peak shifts to lower binding energy by 0.1 eV without evident shape change. For the s4 surface the slight peak widening to high binding energy was attributed to Au–Ti–O bond formation similar to the oxygen interaction with the c(2×2) Sn/Pd(110) surface [9]. The shoulder at 84 eV for s4 as well as the peak shift to lower binding energy for the s6 sample was explained by Ti–O bond formation at the cost of Au–Ti dissociation. The low binding energy shoulder approaches the energy value of bulk gold. For the s6 sample, the Au $4f_{7/2}$ BE of 84.5 eV is higher than the Au bulk value [10]. We conclude that this Au 4f core level corresponds to the Au–Ti alloy phase, the stoichiometry of which was changed by oxygen adsorption. Similar behaviour was observed in our recent study of oxygen interaction with the Sn/Pd(110) surfaces [9]. The normalized Ti 3p to Au $4f_{7/2}$ area ratio for all Au/Ti(0001) surfaces before and after O_2 adsorption is presented in table 3. Assuming the same information depth (same photon energy and geometry) the ratio indicates the change in the surface and subsurface relative element concentration caused by interaction with oxygen. Apart from sample s3 (no O_2 adsorption), it increases after 10 L O_2 exposure and indicates a redistribution of atoms and an increase of surface Ti atom concentration.

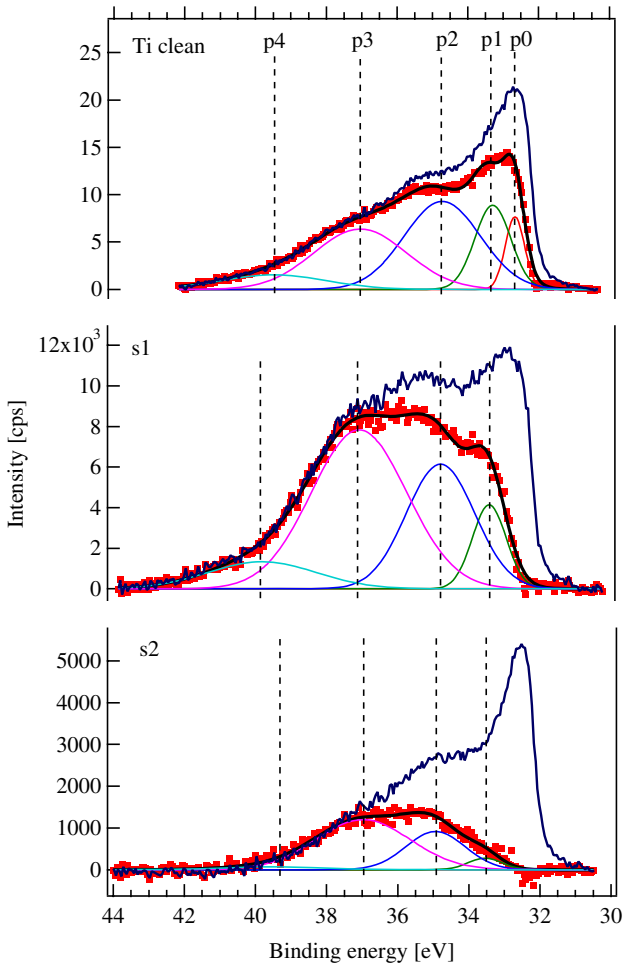

Figure 3. Ti 3p core level after 10 L O_2 adsorption on the clean Ti(0001), s1 and s2 surfaces measured at 148 eV photon energy. Original spectrum is shown together with a fit of the oxygen-induced components for each substrate (see text for details).

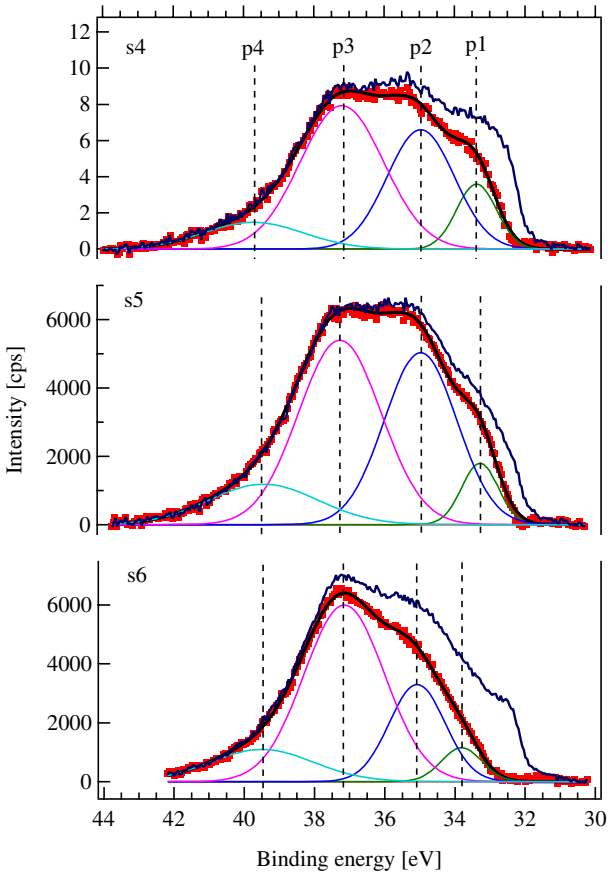

Figure 4. Ti 3p core level after 10 L O_2 adsorption on the clean s4, s5 and s6 surfaces measured at 148 eV photon energy. Original spectrum is shown together with a fit of the oxygen-induced component for each substrate (see text for details).

Table 3. Normalized Ti 3p/Au $4f_{7/2}$ area ratio for Au/Ti(0001) surfaces before and after 10 L O_2 adsorption.

Sample	Ti 3p/Au $4f_{7/2}$	Ti 3p/Au $4f_{7/2}$, O_2 10 L
s1	1.73	3.31
s2	0.17	0.20
s3	0.05	0.05
s4	1.68	3.32
s5	0.59	1.77
s6	0.34	0.84

4. Discussion

As shown above, the main change was observed in the Ti 3p core level after 10 L O_2 exposure of the Au/Ti(0001) surfaces. By peak fitting, several oxygen-induced components were distinguished in the Ti 3p peak, namely TiO, Ti_2O_3, TiO_2 oxide and Ti–OH, labelled p1, p2, p3 and p4 in figures 3 and 4, respectively; their binding energies are shown in table 2. The Ti 3p BE for TiO_2 [6, 7, 11] (see table 2) is the only available reference, which we use to identify p3 as belonging to the TiO_2 oxide. It has a BE in the range from 36.97 to 37.26 eV, and the highest intensity for the O_2-exposed Au/Ti(0001) intermetallic surfaces.

While there is little Ti 3p data available, many more Ti 2p core level photoelectron spectra of oxidized Ti have been published [12–15]. Our assignment of the Ti 3p oxygen-induced features can be linked to this data. Takakuwa *et al* [14] report several Ti oxidation states as the result of exposure of the Ti(0001) surface to O_2 at 473 K, i.e. TiO, Ti_2O_3, Ti_3O_5 and TiO_2 with BE of 1.2, 2.8, 3.9 and 5.2 eV higher than the value of the metallic Ti 2p peak, respectively. Broadening of the metallic Ti 2p core level was also observed during oxidation and was explained by the solid solution of adsorbed oxygen in the crystal together with the possibility of the Ti_2O oxide formation [14]. In our case the BE shifts of the four Ti 3p peaks with respect to the metallic component of the clean Ti(0001) surface were 0.6, 2.05, 4.35 and 6.8 eV, respectively. As noted above the Ti 3p core level shift of 4.35 eV is assigned to TiO_2 [6, 7], i.e. the Ti^{4+} oxidation state. The p1 and p2 peaks, with lower shifts, belong to lower Ti oxides. The p1 peak is attributed to TiO and p2 to Ti_2O_3 (where we cannot exclude a Ti_3O_5 contribution).

The p4 has higher binding energy, but the existence of Ti atoms in higher than +4 oxidation state is unlikely. Thomas *et al* [11] attributed an extra Ti 3p component at BE of about 40 eV to the formation of the Ti–OH species.

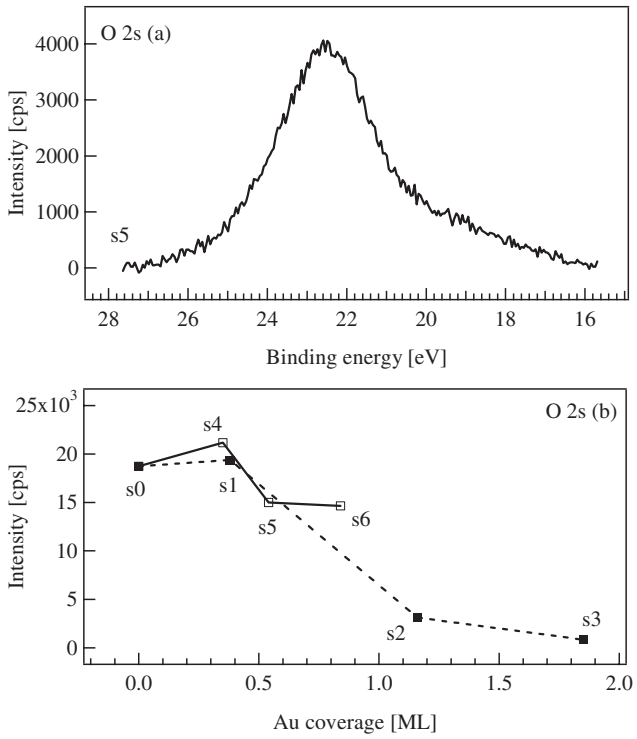

Figure 5. Example of the O 2s core level for the s5 substrate (a), O 2s area plot for all samples and (b) after 10 L O_2 adsorption.

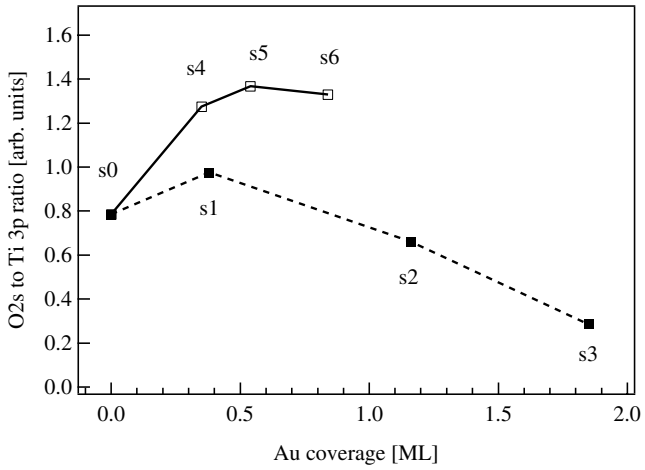

Figure 6. Normalized O 2s to Ti 3p area ratio versus Au coverage.

Taking into account that the residual gas in UHV contains substantial concentrations of hydrogen and H_2O, we follow this assignment of the p4 peak to Ti–OH groups. The component p0 found for the oxygen-exposed Ti(0001) surface at BE close to that of the metallic peak was assigned to chemisorbed oxygen, with a possible contribution of Ti_2O. The core level shifts with respect to the metallic component were found to be lower for the Ti 3p peak compared to the Ti 2p core level.

The O 2s to Ti 3p area ratio (figure 6) is substantially higher for the Au/Ti(0001) intermetallic surfaces compared to the Au adlayers on Ti(0001), where the Au–Ti interaction is limited. Evidently, the amount of adsorbed oxygen

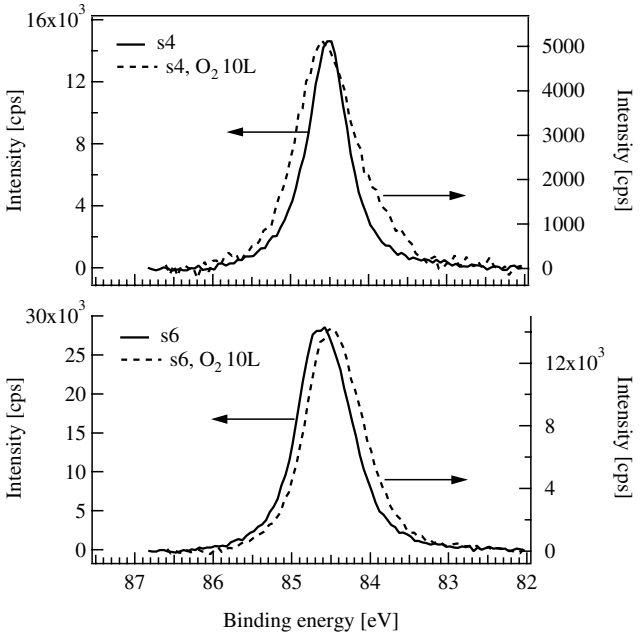

Figure 7. Au $4f_{7/2}$ core level for the s4 and s6 samples before and after oxygen adsorption. Left and right intensity scales correspond to spectra before and after adsorption (indicated by arrows).

is proportional to the number of surface Ti atoms and, as a consequence, depends on the Au–Ti relative surface concentration, mutual interaction and the composition of the subsurface layers.

The biggest change of the Ti 3p to Au $4f_{7/2}$ area ratio after O_2 adsorption was observed for the samples with the highest degree of Au and Ti intermixing, and the ratio increases by a factor of 2 or more for samples s1, s4, s5 and s6. Apparently Ti oxidation is accompanied by Ti atom diffusion from the bulk to the surface enhanced by the presence of the gold atoms, which migrate in the opposite direction. We suggest that oxygen interaction with Au–Ti alloys induces dissociation of the bimetallic bond and redistribution of Au and Ti atoms in the surface region, to minimize the surface energy at 300 K. The fact that the intensity of the Au core levels is always lower after interaction with oxygen confirms the outward diffusion of the Ti atoms in agreement with the work of Zhang *et al* [4] on the thermal oxidation of the gold pre-covered Ti6Al4V alloy and commercially pure Ti at 1120 K.

5. Conclusions

The reaction of oxygen at low pressure with the Au/Ti(0001) surface at 300 K was studied by photoelectron spectroscopy. The main information was obtained from the analysis of the Ti 3p, Au 4f and O 2s core levels, which are shallow peaks with high sensitivity factors under the present experimental conditions. Ti atoms interact with the O_2 and become oxidized while the Au atoms are almost unaffected by a 10 L dose. Oxygen-induced Ti states were examined by fitting of the Ti 3p core level. The Ti atoms in different oxidation states, namely TiO, Ti_2O_3, TiO_2 and Ti–OH, were identified with binding energy shifts of 0.6, 2.05, 4.35 and 6.8 eV with respect to the metallic component of the clean Ti(0001) surface. It was

shown that the amount of adsorbed oxygen is proportional to the number of the top-surface Ti atoms alloyed with gold whereas Ti–O phase formation is accompanied by Au–Ti bond dissociation and Ti outward diffusion.

We have shown that the TiO_2 component dominates for the Au/Ti(0001) intermetallic surfaces compared with the Ti(0001) surface. For the Au/Ti(0001) surfaces the biggest relative TiO_2 contribution to the Ti 2p signal was found for the surface with the thickest Au–Ti subsurface intermetallic film.

Bearing in mind the recent study of O_2 interaction with the Sn/Pd(110) surface [9], we conclude that for easily oxidized metals (sp as in the case of Sn or early transition metals such as Ti) alloying with other metals (transition metals such as Pd or noble metals such as Au) promotes the oxidation, and can be used as a key factor for the well-defined oxide growth especially in nanometre scale devices, by controlling the relative concentration of the metal additives.

Acknowledgments

The Materials Science Beamline is supported by the Ministry of Education of the Czech Republic under grant no. LC06058. We thank our colleagues at Elettra for their help and assistance.

References

[1] Diebold U 2003 *Surf. Sci. Rep.* **48** 53
[2] Liu X, Chu P K and Ding C 2004 *Mater. Sci. Eng.* R **47** 49
[3] Fernández-García M, Martínez-Arias A, Hanson J C and Rodriguez J A 2004 *Chem. Rev.* **104** 4063
[4] Zhang Z X, Dong H, Bell T and Xu B S 2006 *Oxidation Met.* **66** 91
[5] Tsud N, Šutara F, Matolínová I, Veltruská K, Dudr V, Cháb V, Prince K C and Matolín V 2006 *Appl. Surf. Sci.* **252** 5428
[6] Espinós J P, Lassaletta G, Caballero A, Fernández A and González-Elipe A R 1998 *Langmuir* **14** 4908
[7] Bourgeois S, Domenichini B, Šutara F and Matolín V 2008 *Vacuum* **82** 146
[8] Bartkowski S, Neumann M, Kurmaev E Z, Fedorenko V V, Shamin S N, Cherkashenko V M, Nemnonov S N, Winiarski A and Rubie D C 1997 *Phys. Rev.* B **56** 10656
[9] Tsud N, Skála T, Šutara F, Veltruská K, Dudr V, Yoshitake M, Prince K C and Matolín V 2009 *J. Phys.: Condens. Matter* **21** 185011
[10] Chastain J (ed) 1992 *Handbook of X-ray Photoelectron Spectroscopy* (Eden Prairie, MN: Perkin-Elmer Corporation)
[11] Thomas A G, Flavell W R, Mallick A K, Kumarasinghe A R, Tsoutsou D, Khan N, Chatwin C, Rayner S, Smith G C, Stockbauer R L, Warren S, Johal T K, Patel S, Holland D, Taleb A and Wiame F 2007 *Phys. Rev.* B **75** 35105
[12] Lu G, Bernasek S L and Schwartz J 2000 *Surf. Sci.* **458** 80
[13] Takakuwa Y, Ishidzuka S, Yoshigoe A, Teraoka Y, Mizuno Y, Tonda H and Homma T 2003 *Nucl. Instrum. Methods Phys. Res.* B **200** 376
[14] Takakuwa Y, Ishidzuka S, Yoshigoe A, Teraoka Y, Yamauchi Y, Mizuno Y, Tonda H and Homma T 2003 *Appl. Surf. Sci.* **216** 395
[15] Mizuno Y, King F K, Yamauchi Y, Homma T, Tanaka A, Takakuwa Y and Tomose T 2002 *J. Vac. Sci. Technol.* A **20** 1716